Published in "Clinical Cancer Research
doi: 10.1158/1078-0432.CCR-11-302, 2012"
which should be cited to refer to this work.

Inhibition of the Kit ligand/c-Kit axis attenuates metastasis in a mouse model mimicking local breast cancer relapse after radiotherapy

François Kuonen[1,2,*], Julien Laurent[1,*,§], Chiara Secondini[3,§], Girieca Lorusso[1,2,3], Jean-Christophe Stehle[4], Thierry Rausch[4], Eveline Faes-van't Hull[1], Grégory Bieler[1,3], Gian-Carlo Alghisi[1], Reto Schwendener[5], Snezana Andrejevic-Blant[4], René-Olivier Mirimanoff[6], and Curzio Rüegg[1,2,3]

1. Division of Experimental Oncology, Centre Pluridiscipliniaire d'Oncologie (CePO), Centre Hospitalier Universitaire Vaudois (CHUV) and University of Lausanne (UNIL). Faculty of Biology and Medicine, Lausanne, Switzerland;

2. National Center for Competence in Research (NCCR) Molecular Oncology, Swiss Institute of Experimental Cancer Research, Ecole Polytechnique Fédérale de Lausanne (ISREC-EPFL), Lausanne, Switzerland;

3. Chair of Pathology, Department of Medicine, Faculty of Science, University of Fribourg, Fribourg, Switzerland;

4. Institute of Pathology, Centre Hospitalier Universitaire Vaudois (CHUV) and University of Lausanne (UNIL), Lausanne, Switzerland;

5. Institute of Molecular Cancer Research, University of Zurich, Zurich, Switzerland

6. Department of Radio-Oncology, Centre Hospitalier Universitaire Vaudois (CHUV) and University of Lausanne (UNIL), Lausanne, Switzerland.

Corresponding author: Curzio Rüegg, Chair of Pathology, Department of Medicine, Faculty of Science, University of Fribourg, 1 Rue Albert Gockel, CH-1700 Fribourg, Switzerland; Phone: +41-26-300-8766; Fax; +41-26-300-9732.

Conflicts of interest : CR is cofounder and stock holder of Diagnoplex SA. All other authors declare no conflicts of interest.

* Current addresses: F.K., Department of Dermatology, CHUV, Lausanne, Switzerland; J.L., Global Clinical Development Unit – Oncology Merck KGaA, D-64293 Darmstadt.

§ These authors contributed equally to the work.

Abstract

Purpose: Local breast cancer relapse after breast-saving surgery and radiotherapy is associated with increased risk of distant metastasis formation. The mechanisms involved remain largely elusive. We used the well-characterized 4T1 syngeneic, orthotopic breast cancer model to identify novel mechanisms of post-radiation metastasis.

Experimental Design: 4T1 cells were injected in 20 Gy pre-irradiated mammary tissue, to mimic post-radiation relapses, or in non-irradiated mammary tissue, as control, of immunocompetent BALB/c mice. Molecular, biochemical, cellular, histological analyses, adoptive cell transfer, genetic and pharmacological interventions were performed.

Results: Tumors growing in pre-irradiated mammary tissue had reduced angiogenesis, were more hypoxic, invasive and metastatic to lung and lymph nodes compared to control tumors. Increased metastasis involved the mobilization of $CD11b^{+}c\text{-}Kit^{+}Ly6G^{high}Ly6C^{low}(Gr1^{+})$ myeloid cells through the HIF1-dependent expression of KitL by hypoxic tumor cells. KitL-mobilized myeloid cells homed to primary tumors and pre-metastatic lungs, to give rise to $CD11b^{+}c\text{-}Kit^{-}$ cells. Pharmacological inhibition of HIF1, silencing of KitL expression in tumor cells and inhibition of c-Kit with an anti-c-Kit blocking antibody or with a tyrosine kinase inhibitor, prevented the mobilization of $CD11b^{+}c\text{-}Kit^{+}$ cells and attenuated metastasis. C-Kit inhibition was also effective in reducing mobilization of $CD11b^{+}c\text{-}Kit^{+}$ cells and inhibiting lung metastasis after irradiation of established tumors.

Conclusions: Our work defines KitL/c-Kit as a previously unidentified axis critically involved in promoting metastasis of 4T1 tumors growing in pre-irradiated mammary tissue. Pharmacological inhibition of this axis represents a potential therapeutic

strategy to prevent metastasis in breast cancer patients with local relapses after radiotherapy.

Translational relevance

Patients with local breast cancer relapse after conservative breast cancer surgery and radiotherapy have an increased risk of metastasis formation. To date there is no effective therapy to prevent progression to metastasis in these patients. Using a well-characterized model of murine breast cancer, we identified the KitL/c-Kit axis as being critically involved in promoting metastasis of tumors growing in pre-irradiated mammary tissue. The mechanisms involve KitL-dependent mobilization of metastasis-promoting $CD11b^{+}$c-$Kit^{+}Ly6G^{high}Ly6C^{low}(Gr1^{+})$ myeloid cells. These findings have two immediate translational implications. Firstly, circulating $CD11b^{+}$c-Kit^{+} cells might be used as biomarkers to identify patients at risk for post-radiation metastasis. Secondly, inhibition of c-Kit could be an attractive approach to improve efficacy of radiotherapy or to prevent metastasis in breast cancer patients with local relapses after radiotherapy. Translational studies aimed at validating these results in patients are warranted.

Key Words. Breast cancer, radiotherapy, metastasis, c-Kit, tyrosine kinase inhibitor

Introduction

Adjuvant radiotherapy provides survival advantages compared to surgery alone and it is nowadays standard treatment in the management of several cancers, including breast cancer (1). Despite progress in the delivery mode, loco-regional post-radiotherapy relapses still occur in a fraction of treated patients. Relapses occurring within a pre-irradiated area are associated with an increased risk of local invasion, metastasis formation and poor prognosis compared to relapses occurring outside of the irradiated area including in breast (2) and head and neck cancers (3). Experimental evidence supports these clinical observations. In murine xenograft models, tumors developing within pre-irradiated beds are more invasive and metastatic compared to tumors growing outside irradiated beds, a condition also referred to as tumor bed effect (4, 5). One common feature of the tumor bed effect is the appearance of hypoxia (6-8), which is likely due to the inhibition of angiogenesis by ionizing radiations (9, 10). Tumor hypoxia is associated with increased invasiveness, greater risk of metastasis formation and shorter disease-free survival in different human tumors, including soft tissue sarcoma (11), head and neck (12), cervical (13) and breast cancers (14). In spite of its clinical relevance, the cellular and molecular mechanisms underlying the tumor bed effect are still not fully elucidated. Using human melanoma cells grafted in pre-irradiated, immunosuppressed mice, Rofstad and colleagues demonstrated that interleukin-8 (IL-8) and the receptor of urokinase-type plasminogen activator (uPAR) are important mediators of the tumor bed effect in this model (8, 15). We have previously shown that the matricellular protein cysteine rich protein 61 (CYR61) and integrin $\alpha V\beta 5$ cooperate to promote invasion and metastasis of squamous cell carcinoma and colorectal adenocarcinoma growing subcutaneously in pre-irradiated, immunosuppressed mice (7).

Kit ligand (KitL), also known as stem cell factor (SCF) or Steele factor, is a cell surface protein existing in two alternatively spliced isoforms (16). One isoform contains a cleavage site that allows protease-mediated shedding from the cell surface as homodimeric soluble KitL, while the other one cannot be released and remains associated to the cell surface (17). KitL binds to the tyrosine kinase receptor c-Kit (18). During development KitL and c-Kit play critical roles in guiding cell migration, in particular at sites of hematopoiesis, in the central nervous system, in the gut and in the skin (melanogenesis) (19). C-Kit is down-regulated in adult tissues, except in hematopoietic stem/progenitor cells in the bone marrow, in melanocytes and in mast cells. Accordingly, after development the KitL/c-Kit axis is essential for the maintenance of hematopoiesis and for mast cell survival and function in peripheral tissues (20). In cancer c-Kit acts as oncogene in several tumors, in particular gastrointestinal stromal tumors (GIST), mastocytosis and melanoma (20), through activating mutations in the extracellular or intracellular domain (18), or through an autocrine KitL/c-Kit loop (21). The KitL also activates tissue-resident mast cells to generate a tumor-promoting angiogenic microenvironment (22, 23). A role of the KitL/c-Kit axis in metastasis formation, however, has remained unexplored.

In this work we investigated cellular and molecular mechanisms underlying the tumor bed effect in breast cancer by using a model mimicking local relapse after radiotherapy. Presented results identify the KitL/c-Kit axis as a previously unsuspected mediator of metastasis in breast cancer.

Materials and Methods

Antibodies, reagents and cell lines. Biotinylated rat anti-CD31 (MEC 13.3), FITC-conjugated anti-CD11b (M1/70), PE-conjugated anti-c-Kit (2B8), APC-conjugated anti-CXCR4 (2B11), PE-conjugated rat IgG2b isotype control (A95-1) and CD16/CD32 Fc-Block (2.4G2) were purchased from BD Biosciences (Basel, Switzerland). PE-conjugated anti-CCR5 (HM-CCR5), unconjugated and PercP-conjugated anti-F4/80 (BM8), PercP-conjugated anti-Sca1 (D7), Pacific blue-conjugated anti-CD31 (390), unconjugated and Pacific blue-conjugated anti-CD11b (M1/70), APC-conjugated anti-CD45 (30-F11), FITC-conjugated anti-CD11c (N418), FITC-conjugated Harmenian Hamster IgG2 isotype control (HTK888), Alexa Fluor 647-conjugated anti-Ly-6G, PerCP-conjugated anti-Ly-6C, PE-conjugated hamster IgG (HTK888), PercP-conjugated rat IgG2a (RTK2758) and Pacific blue-conjugated rat IgG2a (RTK2758) isotype controls were purchased from Biolegend (San Diego, CA). Pacific blue-conjugated anti-CD45 (30-F11), APC-conjugated anti-Gr-1 (RB6-8C5), APC-conjugated anti-CD123 (5B11), APC-conjugated rat IgG2a isotype control and APC-conjugated rat IgG2b isotype control were purchased from eBioscience (San Diego, CA). APC-conjugated anti-VEGF-R1 (141522) was purchased from R&D (Abingdon, UK). LIVE/DEAD fixable near-IR dead cell stain kit and 4',6-diamidino-2-phenylindole (DAPI) were purchased from Invitrogen (Basel, Switzerland). The hydroxyprobe-1 kit for detection of tissue hypoxia was obtained from HPI Inc, Burlington, MA. 4T1 cell line was generously provided by Dr. Fred R. Miller (Michigan Cancer Foundation, Detroit, MI) (24). HEPA-1 C1C7 and HEPA-1 C4 cells were obtained from Dr. Isabelle Desbaillet-Hakimi (CHUV, Lausanne, Switzerland). For all experiments, cells were grown in DMEM high glucose supplemented with 10% fetal

calf serum and 1% Penicillin/Streptomycin (all purchased from Invitrogen, Basel, Switzerland). For hypoxic treatment, cells were placed into a hypoxic chamber at 0.1% O_2. HIF1-inhibitor NSC-134754 (Developmental Therapeutics Program, NCI/NIH) was used at 1μM.

Mouse model, irradiation and drug treatment. Adult (5-7 weeks of age) BALB/c female mice (Charles River Laboratories, Maastricht, The Netherlands) were used as host animals for grafted tumors. BALB/c mice expressing GFP under the α-actin promoter were generously provided by Dr. S. Swain (Trudeau Institute, Saranac Lake, NY). Primary tumors were initiated by the injection of 4T1 tumor cells ($5x10^4$ cells/mouse) into the right 4^{th} mammary gland in 50μl of 1:5 mixture of Matrigel (BD Biosciences) and PBS. Before injection, the 4^{th} mammary gland was locally irradiated with a single 20 Gy dose by using an X-ray unit (PHILIPS, RT 250, Germany), operated at a 125 kV, 20 mA, with a 2 mm Al filter. Drugs were administered as following: Clodrolip: 2 mg/20 g mouse body weight as initial dose, followed by 1 mg for the subsequent doses injected i.p. every 4^{th} day starting from day 6; NSC-134754: 5 mg/kg dose, injected i.p. daily from day 5; ACK2 (Biolegend): 50 μg dose, injected i.p. four times every 3^{rd} day from day 10. Nilotinib (AMN107-AA, kindly provided by Novartis, Basel): 20 mg/kg dose, administered daily by gavage, from day 7. All animal experiments have been subjected to control and authorization by the cantonal veterinary service (Vaud and Fribourg). Tumor volume and lung metastases were assessed as previously described (7). For the quantification of lymphatic and liver metastases, axillary lymph nodes and liver sections were stained with HE and assessed for the presence of metastatic foci. For the irradiation of established tumors, 4T1 tumors were initiated as above, and when they were palpable (day 8

after tumor initiation) they were locally irradiated with the same settings (20 Gy, single dose). ACK2 treatment was performed as above.

Flow cytometry. For flow cytometry on blood circulating cells, 50 µl of fresh blood were collected from the tail vein in 3 µl of 0.5M EDTA. Bone marrow resident cells were collected from femoral bones and filtered to form single-cell suspensions. For flow cytometry analyses on tumors and lungs, mice were perfused with PBS by intracardiac injection. Mammary tissue, tumors and lungs were excised, mechanically disrupted, enzymatically digested and then filtered to obtain single-cell suspensions. Staining and acquisition were done as described (25). Samples were acquired with a FACS LSR II, FACScalibur (Becton-Dickinson, Basel, Switzerland) or MACS Quant Analyzer Miltenyi (Teterow, Germany) and data analyzed using FCS Express Version 3 (De Novo Software, Los Angeles, CA) or FlowJo (Tree Star, Inc.Ashland, OR).

c-Kit$^+$ cell depletion and fluorescence-activated cell sorting. PBMCs were isolated using the Ficoll procedure. To asses the effect of circulating c-Kit$^+$ cells on metastasis, 10x10^6 PBMCs were injected at day 8 and 12 either directly or after depletion of c-Kit$^+$ cells using the EasySep® Magnet procedure according to the manufacturer's instructions (Stemcell Technologies, Grenoble, France). For *in vivo* cell tracking, PBMCs were sorted using FACS Aria (Becton-Dickinson). The purity of the sorted samples was assessed by direct flow cytometry re-analysis and viability of the cells estimated with Trypan blue staining. 2x10^6 c-Kit$^+$ cells were then injected intravenously in 4T1-bearing mice.

Statistical analyses. Statistical comparisons were performed by a two-tailed Student's t test or one-way ANOVA with Bonferroni post-test using Prism 5.0 GraphPad Software (La Jolla, CA). Results were considered to be significant with $p < 0.05$. *, $p < 0.05$; **, $p < 0.01$; ***, $p < 0.001$.

Additional methods are available as supplementary material on line.

Results

Tumors growing in pre-irradiated mammary tissue have decreased vascular density, are more hypoxic, invasive and metastatic

To investigate the effect of mammary tissue irradiation on breast cancer progression, we pre-irradiated the 4th mammary gland of BALB/c mice with 20 Gy X-ray single dose before implanting 4T1 tumor cells (24). While in current clinical practice adjuvant radiotherapy in breast cancer is delivered in fractionated doses, in this model it was not possible to perform multiple irradiations because of technical and ethical issues. Nevertheless, the single X-ray dose was chosen to correspond to the cumulative dose of approximately 60 Gy delivered to breast cancer patients during fractionated therapy (26). Mammary tissue pre-irradiation had no significant effect on 4T1 primary tumor growth (Supplementary Fig. S1A). Tumors growing in a pre-irradiated mammary tissue showed reduced microvascular density, increased hypoxia and necrosis (Fig. 1A), consistent with radiation-induced inhibition of angiogenesis (9, 10). They were also more invasive into the surrounding muscle and fat tissues (Fig. 1B), and more metastatic to ipsilateral axillary lymph nodes (Fig. 1C), lungs (Fig. 1D) and liver (Supplementary Fig. S1B).

These results demonstrate that 4T1 breast tumors growing in a pre-irradiated mammary tissue undergo a tumor bed effect that recapitulates clinically relevant features of breast cancers locally relapsing after radiotherapy.

Tumors growing in pre-irradiated mammary tissue recruit metastasis-promoting CD11b^{+} cells

In tumor growing in pre-irradiated beds we observed a significant increase in the recruitment of $CD11b^+$ myeloid cells, and of two subpopulations thereof, $CD11b^+F4/80^+$ and $CD11b^+Gr1^+$ (Fig. 2A and Supplementary Fig. S2A). Irradiation of the mammary tissue without tumor implantation did not induce recruitment of $CD11b^+$ myeloid cells (Fig. 2A). Enhanced recruitment occurred in the tumor periphery as demonstrated by F4/80 staining (Fig. 2B). Treatment with Clodrolip to deplete phagocytic myeloid cells (27) did not affect primary tumor growth (Supplementary Fig. S2B), but significantly reduced the number of $CD11b^+$ and $F4/80^+$ cells in the tumor (Fig. 2C, Supplementary Fig. S2C, left panel, and S2D), microvascular density (Supplementary Fig. S2C, right panel, and S2D), and lung metastasis formation (Fig. 2D and Supplementary Fig. S2E).

These results demonstrate that mammary tissue irradiation enhances recruitment of $CD11b^+$ cells contributing to lung metastasis formation.

HIF1-dependent Kit ligand expression in hypoxic tumor cells promotes metastasis

Hypoxic tumors can mobilize bone marrow-derived cells by releasing soluble factors (28). We therefore screened for cytokines induced by hypoxia in 4T1 cells and potentially involved in $CD11b^+$ cell mobilization. In addition to VEGF-A and MCP-1, Kit-ligand (KitL) was among the cytokines significantly induced by hypoxia (24 hours, 0.1% O_2) in 4T1 cells *in vitro* at both the mRNA and protein levels (Fig. 3A and Supplementary Fig. S3A). Since bone marrow-derived cells expressing the KitL receptor c-Kit (20) are present in the pre-metastatic niche (29), but the putative role of KitL/c-Kit axis in metastasis formation has not been assessed yet, we decided to focus on KitL. VEGF-A expression was monitored as a control for effective hypoxia

and activity of the HIF1 inhibitor NSC-134754 (30) (Supplementary Fig. S3A and S3B). Inhibition of HIF1 in 4T1 cells by NSC-134754 and genetic deficiency of the β subunit of the HIF complex in HEPA1 cells prevented hypoxia-induced up-regulation of KitL mRNA and protein (Fig. 3A, Supplementary Fig. S3B and S3C). 4T1 tumors growing within a pre-irradiated bed had increased KitL protein (Fig. 3B) and mRNA (Supplementary Fig. S4A) levels, and this increase was blunted by NSC-134754 treatment (Fig. 3B). Mammary tissue irradiation alone did not induce KitL expression (Supplementary Fig. S4B). Plasma levels of KitL were higher in pre-irradiated tumor-bearing mice compared to controls (Fig. 3C) demonstrating systemic release of KitL (31). In contrast, CXCL12, a chemokine previously reported to promote $CD11b^+$ cell recruitment within irradiated tumors (32), was not induced in this model (Supplementary Fig. S4C). Silencing of KitL expression in 4T1 cells through lentiviral–mediated expression of KitL-specific short-hairpin (sh) RNAs (Supplementary Fig. S4D and S4E) suppressed lung metastasis formation of 4T1 tumors growing in pre-irradiated mammary tissue (Fig. 3D), while it did not affect 4T1 tumor cell growth *in vitro* or *in vivo* (Supplementary Fig. S4F and S4G).

These results demonstrate that KitL expression is induced by hypoxia in a HIF1-dependent manner, and that KitL is required for increased metastatic spreading, but not primary growth, of 4T1 tumors implanted in pre-irradiated mammary tissue.

KitL mobilizes $CD11b^+$c-Kit^+ cells

To ascertain cells responding to KitL we set up to identify c-Kit-expressing cells in tumor-bearing mice. C-Kit expression was undetectable on $CD45^-$ and $CD45^+$ cells recovered from primary tumors, while it was detectable at low frequency on bone marrow cells and circulating $CD45^+$ myeloid cells (Fig. 4A and Supplementary Fig.

S5A). C-Kit$^+$ cells were virtually undetectable in the blood of tumor-free mice (Fig. 4B). Circulating c-Kit$^+$ cells in pre-irradiated, tumor-bearing mice expressed CD11b and Gr1 but were negative for F4/80, CCR5, CXCR4, VEGF-R1, Sca1 and CD123 (a marker for mast cells) (33) expression (Supplementary Fig. S5B). Their morphology was consistent with young, immature myeloid cells (Supplementary Fig. S5C). Circulating c-Kit$^+$ cells were unable to form hematopoietic colonies, in contrast to bone marrow-derived c-Kit$^+$ cells (Supplementary Fig. S5D). Further phenotypical analysis revealed that circulating c-Kit$^+$CD11b$^+$ cells were Ly6G^{high} and Ly6C^{low} and CD11c negative (Supplementary Fig. S6A and S6B). Tumor-infiltrating CD11b$^+$ cells were predominantly Ly6G^{high} (Supplementary Fig. S6C). The Ly6G^{high}Ly6C^{low} phenotype is indicative of CD11b$^+$ granulocytic myeloid-derived suppressor cells (MDSC) (34), consistent with the well documented ability of 4T1 tumors to expand and mobilize MDSC (35, 36). Tumors implanted in pre-irradiated mammary tissue, but not mammary tissue irradiation alone, significantly enhanced the frequency of circulating CD11b$^+$c-Kit$^+$ cells, compared to control tumors (Fig. 4B), and KitL silencing in 4T1 tumor cells or systemic administration of NSC-134754 significantly reduced it (Fig. 4C).

Mobilized CD11b$^+$c-Kit$^+$ cells home to tumors and pre-metastatic lungs in a KitL-dependent manner

To monitor the fate of circulating c-Kit$^+$ cells we isolated circulating GFP$^+$CD11b$^+$c-Kit$^+$ cells from tumor-bearing GFP-BALB/c mice (over 95% enriched, not shown) and injected them into recipient BALB/c mice bearing 4T1 tumors implanted in pre-irradiated mammary tissue. Six hours after intravenous injection, GFP$^+$CD11b$^+$ cells were detectable in the blood and in tumor tissue, however, only

approximately 25% and none of the transferred cells retained c-Kit expression, respectively (Fig. 5A). KitL silencing in 4T1 tumors significantly reduced radiation-induced recruitment of $CD11b^+$ cells to primary tumors (Fig. 5B). In a second adoptive transfer experiment we demonstrated that $GFP^+CD11b^+c\text{-}Kit^+$ cells also home to lungs of BALB/c recipient mice bearing tumors growing in pre-irradiated mammary tissue, with only approximately 25% of them retaining c-Kit expression (Fig. 5C). $C\text{-}Kit^+$ cells were also present in lungs of tumor-bearing mice 15 days after tumor implantation, and their frequency increased in mice bearing tumors growing in pre-irradiated beds compared to non-irradiated controls. This increase was blunted by KitL silencing in tumor cells (Figure 5D).

These results indicate that tumor-derived KitL mobilizes $CD11b^+c\text{-}Kit^+$ cells to home to primary tumors and pre-metastatic lungs, but once recruited the rapidly lose c-Kit expression.

Mobilized $CD11b^+c\text{-}Kit^+$ cells promote lung metastasis

To obtain evidence whether tumor-mobilized $c\text{-}Kit^+$ myeloid cells promote lung metastasis, we isolated peripheral blood mononuclear cells (PBMCs) from pre-irradiated tumor-bearing mice, and injected either the total PBMCs or PBMCs depleted of $c\text{-}Kit^+$ cells (Supplementary Fig. S7A) into non-irradiated tumor-bearing mice and monitored lung metastasis formation. Transfer of total PBMCs increased lung metastasis by about 5 fold, while transfer of $c\text{-}Kit^+$ cell-depleted PBMCs resulted in a significantly reduced increase in lung metastasis (Fig. 6A). No effects on primary tumor growth were observed (Supplementary Fig. S7B).

These results indicate that mobillized $CD11b^+c\text{-}Kit^+$ cells significantly contribute to promote lung metastasis.

c-Kit inhibition reduces mobilization of CD11b$^+$c-Kit$^+$ cells and attenuates lung metastases

To test whether inhibition of c-Kit impinges on lung metastasis formation, we treated pre-irradiated, tumor-bearing mice with the anti-c-Kit blocking antibody ACK2 (Ref. (37)). ACK2 treatment suppressed radiation-induced mobilization of c-Kit$^+$ cells, accumulation of CD11b$^+$ cells in primary tumors (Fig. 6B) and attenuated lung metastasis formation by approximately 50% (Fig. 6C, upper panel). Treatment with nilotinib (AMN107-AA), a tyrosine kinase inhibitor that effectively block c-Kit activity (38), suppressed lung metastasis formation to a similar extent (Fig. 6C, lower panel). ACK2 or nilotinib treatments did not impinge on primary tumor growth (Supplementary Fig. S7C and S7D). To assess whether this mechanism may also apply to irradiated tumors, we irradiated established 4T1 tumors. Irradiation significantly delayed tumor growth and increased lung metastasis (Supplementary Fig. S8A and S8B). Treatment with ACK2 reduced the frequency of circulating CD11b$^+$c-Kit$^+$ cells and the number of lung metastases (Supplementary Fig. S8C and S8D) without impinging on tumor growth (Supplementary Fig. S8E).

These results demonstrate that c-Kit activity is critically involved in mediating the mobilization of CD11b$^+$c-Kit$^+$ cells and in promoting lung metastasis formation of 4T1 tumors growing in pre-irradiated mammary tissue or after tumor irradiation.

Discussion

In spite of their clinical relevance, the cellular and molecular mechanisms mediating metastasis of tumors locally relapsing after radiotherapy are still largely elusive. In this work we using the well-characterized 4T1 murine breast cancer

model, we discovered a novel mechanism promoting metastasis of breast cancer growing in a pre-irradiated bed.

The main novel finding is the identification of the KitL/c-Kit axis as a crucial element of this mechanism. We show that tumors growing in a pre-irradiated bed are poorly vascularized and hypoxic, and that hypoxia induces HIF1-dependent KitL expression by tumor cells. Released KitL mobilizes $CD11b^{+}$c-$Kit^{+}Ly6G^{high}Ly6C^{low}$ ($Gr1^{+}$) myeloid cells, which recruit to primary tumors and to lungs and facilitate lung metastasis formation. Expression of KitL in peri-necrotic tumor regions was reported in human cancers, including breast cancer, and correlates with progression (39). The tumor-promoting effect of KitL was considered due to KitL stimulating c-Kit^{+} tumor cells or c-Kit^{+} endothelial cells and mast cells, resulting in enhanced cell growth (40), angiogenesis (41) and immunosuppression (42).

The second main finding is the identification of $CD11b^{+}$c-$Kit^{+}Ly6G^{high}Ly6C^{low}$ (and $F4/80^{-}CCR5^{-}CXCR4^{-}Flt1^{-}CD123^{-}$) cells as novel $CD11b^{+}$ sub-population with metastasis-promoting activity. Recruited $CD11b^{+}$c-Kit^{+} cells rapidly lose c-Kit from their surface, to give rise to $CD11b^{+}$c-Kit^{-} cells, which may be the actual cells promoting metastasis. This is consistent with the enriched presence of $CD11b^{+}$ cells at the invasive tumor front and the observed reduced metastasis formation following depletion by Clodrolip. $CD11b^{+}$ cells are known to promote tumor growth, invasion and metastasis through multiple mechanisms, including angiogenesis (43), vasculogenesis (10, 32), immunosuppression (44), lymphangiogenesis (45) and tumor cell motility (46). Taken together, our results identify KitL as a factor inducing the mobilization and recruitment to tumors and lungs of $CD11b^{+}$ myeloid cells, in addition to already identified factors, such as including VEGF-A (47), CXCL12 (48), CXCL5 (46) and PlGF (49). We are currently investigating the mechanisms by which

$CD11b^+c\text{-}Kit^+$ cells (and $CD11b^+$ $c\text{-}Kit^-$ cells derived thereof) promote metastasis. The reduced microvascular density induced by Clodrolip treatments in tumors growing in a pre-irradiated bed suggests that these cells possess vessel-forming properties, possibly by vasculogenesis, as recently reported (32). The $Ly6G^{high}Ly6C^{low}$ phenotype consistent with a granulocytic MDSC population (34) also raises the possibility that immunosuppressive effects might contribute to promote metastasis.

These results have two immediate translational implications. Firstly, they identify circulating $CD11b^+c\text{-}Kit^+$ cells as candidate biomarkers to stratify patients at risk for post-radiation metastasis. We have attempted to validate this hypothesis using archive material, but the limited number of cases identified and restrictive local ethical regulations hindered this approach. Preliminary analyses in humans indicate that $CD11b^+c\text{-}Kit^+$ are present at low frequency in the peripheral blood of healthy volunteers, and at higher frequency in patients with metastatic breast cancer.

Secondly, they point to the KitL/c-Kit axis as a potential therapeutic target to prevent metastasis of post-radiation breast cancer relapses. C-Kit inhibition by tyrosine kinase inhibitors (TKI) is already used to treat cancers with uncontrolled c-Kit activity (50) (due to c-Kilt overexpression, mutational activation or KitL overexpression), including GIST (51) and melanoma (52). Here, stable silencing of KitL in 4T1 tumor cells, selective c-Kit inhibition by the ACK2 mAb and treatment with nilotinib, a clinically approved TKI that effectively block c-Kit activation (38), all reduced metastasis of tumors growing in a pre-irradiated mammary tissue. C-Kit inhibition also reduced lung metastasis formation of 4T1 tumor that were treated with radiotherapy. Based on these findings, inhibition of c-Kit should be explored as a possible adjuvant approach in patients with local recurrences after radiotherapy and at increased risk for metastatic progression. It is important to note that these findings

are based on one breast cancer cell line only, 4T1. This line is known to induce an unusually strong mobilization of MDSC, which may not occur in all breast cancer models. It will also be important to ascertain whether in human breast cancer this mechanism is common to all breast cancer types, or whether it is specific for a particular breast cancer subtype. To this purpose we are interrogating additional experimental breast cancer models and initiating a clinical study to monitor the frequency of circulating $CD11b^{+}c\text{-}Kit^{+}$ cells in breast cancer patients, before, during and after surgery/radiotherapy. Monitoring $CD11b^{+}c\text{-}Kit^{+}$ cells in the circulation might also be a simple strategy to identify patients with an active KitL/c-Kit axis that may benefit from c-Kit inhibition.

Taken together we have demonstrated that hypoxic breast tumors growing in a pre-irradiated environment mobilize $CD11b^{+}c\text{-}Kit^{+}Ly6G^{high}Ly6C^{low}$ granulocytic MDSC through HIF1-mediated KitL release. These observations extend our understanding of the mechanisms of metastasis of tumors growing in a pre-irradiated bed by implicating for the first time the KitL/c-Kit axis in this effect (Fig. 6D). Translational studies aimed at validating these results in patients are warranted.

Acknowledgments

We thank Drs. F.R. Miller, S. Swain, L. Naldini, R. Iggo, and A. Follenzi for providing cells, mice, or lentiviral vectors. We also thank Drs. C. Bourquin and T. Herbst for assistance with FACS analysis and discussion. We thank Dr. P. Manley, for discussion and providing nilotinib. This work was supported by the European Union under the auspices of the FP7 collaborative project TuMIC, contract no. HEALTH-F2-2008-201662 (to C.R.); The Molecular Oncology Program of the National Center of Competence in Research (NCCR), a research instrument of the Swiss National Science Foundation (to C.R.); A collaborative research project (CCRP) of Oncosuisse (OCS-01812-12-2005) (to C.R.); A Swiss National Science Foundation grant (31003A_135738) (to C.R.); The ISREC foundation (to C.R.), A MD-PhD fellowship from Oncosuisse (to F.K.).

References

1. Fisher B, Anderson S, Redmond CK, Wolmark N, Wickerham DL, Cronin WM. Reanalysis and results after 12 years of follow-up in a randomized clinical trial comparing total mastectomy with lumpectomy with or without irradiation in the treatment of breast cancer. N Engl J Med 1995;333: 1456-61.
2. Vicini FA, Kestin L, Huang R, Martinez A. Does local recurrence affect the rate of distant metastases and survival in patients with early-stage breast carcinoma treated with breast-conserving therapy? Cancer 2003;97: 910-9.
3. Vikram B, Strong EW, Shah JP, Spiro R. Failure in the neck following multimodality treatment for advanced head and neck cancer. Head Neck Surg 1984;6: 724-9.
4. Milas L, Hirata H, Hunter N, Peters LJ. Effect of radiation-induced injury of tumor bed stroma on metastatic spread of murine sarcomas and carcinomas. Cancer Res 1988;48: 2116-20.
5. Camplejohn RS, Penhaligon M. The tumour bed effect: a cell kinetic and histological investigation of tumours growing in irradiated mouse skin. Br J Radiol 1985;58: 443-51.
6. Penhaligon M, Courtenay VD, Camplejohn RS. Tumour bed effect: hypoxic fraction of tumours growing in preirradiated beds. Int J Radiat Biol Relat Stud Phys Chem Med 1987;52: 635-41.
7. Monnier Y, Farmer P, Bieler G, Imaizumi N, Sengstag T, Alghisi GC*, et al.* CYR61 and alphaVbeta5 integrin cooperate to promote invasion and metastasis of tumors growing in preirradiated stroma. Cancer Res 2008;68: 7323-31.

8. Rofstad EK, Mathiesen B, Henriksen K, Kindem K, Galappathi K. The tumor bed effect: increased metastatic dissemination from hypoxia-induced up-regulation of metastasis-promoting gene products. Cancer Res 2005;65: 2387-96.
9. Imaizumi N, Monnier Y, Hegi M, Mirimanoff RO, Ruegg C. Radiotherapy suppresses angiogenesis in mice through TGF-betaRI/ALK5-dependent inhibition of endothelial cell sprouting. PLoS One 2010;5: e11084.
10. Ahn GO, Tseng D, Liao CH, Dorie MJ, Czechowicz A, Brown JM. Inhibition of Mac-1 (CD11b/CD18) enhances tumor response to radiation by reducing myeloid cell recruitment. Proc Natl Acad Sci U S A 2010;107: 8363-8.
11. Brizel DM, Scully SP, Harrelson JM, Layfield LJ, Bean JM, Prosnitz LR*, et al.* Tumor oxygenation predicts for the likelihood of distant metastases in human soft tissue sarcoma. Cancer Res 1996;56: 941-3.
12. Brizel DM, Dodge RK, Clough RW, Dewhirst MW. Oxygenation of head and neck cancer: changes during radiotherapy and impact on treatment outcome. Radiother Oncol 1999;53: 113-7.
13. Hockel M, Schlenger K, Aral B, Mitze M, Schaffer U, Vaupel P. Association between tumor hypoxia and malignant progression in advanced cancer of the uterine cervix. Cancer Res 1996;56: 4509-15.
14. Chaudary N, Hill RP. Hypoxia and metastasis in breast cancer. Breast Dis 2006;26: 55-64.
15. Rofstad EK, Mathiesen B, Galappathi K. Increased metastatic dissemination in human melanoma xenografts after subcurative radiation treatment: radiation-induced increase in fraction of hypoxic cells and hypoxia-induced up-regulation of urokinase-type plasminogen activator receptor. Cancer Res 2004;64: 13-8.

16. Besmer P. The kit ligand encoded at the murine Steel locus: a pleiotropic growth and differentiation factor. Curr Opin Cell Biol 1991;3: 939-46.
17. Anderson DM, Williams DE, Tushinski R, Gimpel S, Eisenman J, Cannizzaro LA*, et al.* Alternate splicing of mRNAs encoding human mast cell growth factor and localization of the gene to chromosome 12q22-q24. Cell Growth Differ 1991;2: 373-8.
18. Liu H, Chen X, Focia PJ, He X. Structural basis for stem cell factor-KIT signaling and activation of class III receptor tyrosine kinases. EMBO J 2007;26: 891-901.
19. Besmer P, Manova K, Duttlinger R, Huang EJ, Packer A, Gyssler C*, et al.* The kit-ligand (steel factor) and its receptor c-kit/W: pleiotropic roles in gametogenesis and melanogenesis. Dev Suppl 1993: 125-37.
20. Pittoni P, Piconese S, Tripodo C, Colombo MP. Tumor-intrinsic and -extrinsic roles of c-Kit: mast cells as the primary off-target of tyrosine kinase inhibitors. Oncogene 2011;30: 757-69.
21. Stanulla M, Welte K, Hadam MR, Pietsch T. Coexpression of stem cell factor and its receptor c-Kit in human malignant glioma cell lines. Acta Neuropathol 1995;89: 158-65.
22. Crivellato E, Nico B, Ribatti D. Mast cells and tumour angiogenesis: new insight from experimental carcinogenesis. Cancer Lett 2008;269: 1-6.
23. Coussens LM, Raymond WW, Bergers G, Laig-Webster M, Behrendtsen O, Werb Z*, et al.* Inflammatory mast cells up-regulate angiogenesis during squamous epithelial carcinogenesis. Genes Dev 1999;13: 1382-97.

24. Aslakson CJ, Miller FR. Selective events in the metastatic process defined by analysis of the sequential dissemination of subpopulations of a mouse mammary tumor. Cancer Res 1992;52: 1399-405.
25. Kuonen F, Touvrey C, Laurent J, Ruegg C. Fc block treatment, dead cells exclusion, and cell aggregates discrimination concur to prevent phenotypical artifacts in the analysis of subpopulations of tumor-infiltrating CD11b(+) myelomonocytic cells. Cytometry A 2010.
26. Barton M. Tables of equivalent dose in 2 Gy fractions: a simple application of the linear quadratic formula. Int J Radiat Oncol Biol Phys 1995;31: 371-8.
27. Zeisberger SM, Odermatt B, Marty C, Zehnder-Fjallman AH, Ballmer-Hofer K, Schwendener RA. Clodronate-liposome-mediated depletion of tumour-associated macrophages: a new and highly effective antiangiogenic therapy approach. Br J Cancer 2006;95: 272-81.
28. Murdoch C, Muthana M, Coffelt SB, Lewis CE. The role of myeloid cells in the promotion of tumour angiogenesis. Nat Rev Cancer 2008;8: 618-31.
29. Kaplan RN, Riba RD, Zacharoulis S, Bramley AH, Vincent L, Costa C*, et al.* VEGFR1-positive haematopoietic bone marrow progenitors initiate the pre-metastatic niche. Nature 2005;438: 820-7.
30. Chau NM, Rogers P, Aherne W, Carroll V, Collins I, McDonald E*, et al.* Identification of novel small molecule inhibitors of hypoxia-inducible factor-1 that differentially block hypoxia-inducible factor-1 activity and hypoxia-inducible factor-1alpha induction in response to hypoxic stress and growth factors. Cancer Res 2005;65: 4918-28.
31. Broudy VC. Stem cell factor and hematopoiesis. Blood 1997;90: 1345-64.

32. Kioi M, Vogel H, Schultz G, Hoffman RM, Harsh GR, Brown JM. Inhibition of vasculogenesis, but not angiogenesis, prevents the recurrence of glioblastoma after irradiation in mice. J Clin Invest 2010;120: 694-705.
33. Schernthaner GH, Hauswirth AW, Baghestanian M, Agis H, Ghannadan M, Worda C*, et al.* Detection of differentiation- and activation-linked cell surface antigens on cultured mast cell progenitors. Allergy 2005;60: 1248-55.
34. Youn JI, Nagaraj S, Collazo M, Gabrilovich DI. Subsets of myeloid-derived suppressor cells in tumor-bearing mice. J Immunol 2008;181: 5791-802.
35. Sinha P, Clements VK, Fulton AM, Ostrand-Rosenberg S. Prostaglandin E2 promotes tumor progression by inducing myeloid-derived suppressor cells. Cancer Res 2007;67: 4507-13.
36. Younos I, Donkor M, Hoke T, Dafferner A, Samson H, Westphal S*, et al.* Tumor- and organ-dependent infiltration by myeloid-derived suppressor cells. Int Immunopharmacol 2011;11: 816-26.
37. Torihashi S, Nishi K, Tokutomi Y, Nishi T, Ward S, Sanders KM. Blockade of kit signaling induces transdifferentiation of interstitial cells of cajal to a smooth muscle phenotype. Gastroenterology 1999;117: 140-8.
38. Manley PW, Drueckes P, Fendrich G, Furet P, Liebetanz J, Martiny-Baron G*, et al.* Extended kinase profile and properties of the protein kinase inhibitor nilotinib. Biochim Biophys Acta 2010;1804: 445-53.
39. Sihto H, Tynninen O, Halonen M, Puputti M, Karjalainen-Lindsberg ML, Kukko H*, et al.* Tumour microvessel endothelial cell KIT and stem cell factor expression in human solid tumours. Histopathology 2009;55: 544-53.

40. Lefevre G, Glotin AL, Calipel A, Mouriaux F, Tran T, Kherrouche Z*, et al.* Roles of stem cell factor/c-Kit and effects of Glivec/STI571 in human uveal melanoma cell tumorigenesis. J Biol Chem 2004;279: 31769-79.
41. Sun L, Hui AM, Su Q, Vortmeyer A, Kotliarov Y, Pastorino S*, et al.* Neuronal and glioma-derived stem cell factor induces angiogenesis within the brain. Cancer Cell 2006;9: 287-300.
42. Huang B, Lei Z, Zhang GM, Li D, Song C, Li B*, et al.* SCF-mediated mast cell infiltration and activation exacerbate the inflammation and immunosuppression in tumor microenvironment. Blood 2008;112: 1269-79.
43. De Palma M, Venneri MA, Galli R, Sergi Sergi L, Politi LS, Sampaolesi M*, et al.* Tie2 identifies a hematopoietic lineage of proangiogenic monocytes required for tumor vessel formation and a mesenchymal population of pericyte progenitors. Cancer Cell 2005;8: 211-26.
44. Marigo I, Dolcetti L, Serafini P, Zanovello P, Bronte V. Tumor-induced tolerance and immune suppression by myeloid derived suppressor cells. Immunol Rev 2008;222: 162-79.
45. Zumsteg A, Baeriswyl V, Imaizumi N, Schwendener R, Ruegg C, Christofori G. Myeloid cells contribute to tumor lymphangiogenesis. PLoS One 2009;4: e7067.
46. Yang L, Huang J, Ren X, Gorska AE, Chytil A, Aakre M*, et al.* Abrogation of TGF beta signaling in mammary carcinomas recruits Gr-1+CD11b+ myeloid cells that promote metastasis. Cancer Cell 2008;13: 23-35.
47. Lewis JS, Landers RJ, Underwood JC, Harris AL, Lewis CE. Expression of vascular endothelial growth factor by macrophages is up-regulated in poorly vascularized areas of breast carcinomas. J Pathol 2000;192: 150-8.

48. Du R, Lu KV, Petritsch C, Liu P, Ganss R, Passegue E*, et al.* HIF1alpha induces the recruitment of bone marrow-derived vascular modulatory cells to regulate tumor angiogenesis and invasion. Cancer Cell 2008;13: 206-20.
49. Fischer C, Jonckx B, Mazzone M, Zacchigna S, Loges S, Pattarini L*, et al.* Anti-PlGF inhibits growth of VEGF(R)-inhibitor-resistant tumors without affecting healthy vessels. Cell 2007;131: 463-75.
50. Lennartsson J, Ronnstrand L. The stem cell factor receptor/c-Kit as a drug target in cancer. Curr Cancer Drug Targets 2006;6: 65-75.
51. Liegl-Atzwanger B, Fletcher JA, Fletcher CD. Gastrointestinal stromal tumors. Virchows Arch 2010;456: 111-27.
52. Smalley KS, Sondak VK, Weber JS. c-KIT signaling as the driving oncogenic event in sub-groups of melanomas. Histol Histopathol 2009;24: 643-50.

Figure legends

Figure 1. Breast cancer cells growing in a pre-irradiated mammary tissue are highly invasive and metastatic. A, 4T1-derived tumors growing in a pre-irradiated mammary tissue had reduced microvascular density (MVD; CD31 staining, *red*; bar: 100 μm), were more hypoxic (pimonidazole staining, *brown*; bar: 100 μm) and necrotic (HE; bar: 1 mm) compared to tumors growing in non-irradiated tissue (0 Gy). B, 4T1 tumors developing in pre-irradiated mammary tissue (20 Gy) were more invasive into fat (F) and muscle (M) tissues compared to control tumors (0 Gy) (bar: 100 μm). C, 4T1 tumors developing in pre-irradiated mammary tissue (20 Gy) were more metastatic to ipsilateral lymph nodes compared to control tumors (0 Gy). A representative metastatic lymph node is shown in HE staining (bar: 50 μm). D, 4T1 tumors growing in pre-irradiated mammary tissue (20 Gy) were highly metastatic to lungs compared to control tumors (0 Gy). Representative HE stained sections of lungs are shown (bar: 1 mm). Tumors were assessed at day 10 and metastases were at day 24 after tumor initiation. *$p < 0.05$ and **$p < 0.01$, $n \geq 5$ mice per group. Results represent mean values ± SEM.

Figure 2. Mobilized myeloid cells promote lung metastasis. A, 4T1 tumors growing in a pre-irradiated mammary tissue (20 Gy) were more densely infiltrated by $CD11b^+$ cells compared to control tumors (0 Gy) and to tumor-free mammary fat pads. B, Myeloid cells (detected by F4/80 staining) accumulated preferentially at the periphery rather than in the center of tumors growing in pre-irradiated mammary tissue (20 Gy) compared to control tumors (0 Gy) (bars: 50 μm). Bottom graph shows data quantification (TC, tumor center; TP, tumor periphery). C, Clodrolip treatment

(15 days after tumor implantation) depleted $CD11b^+$ cells from 4T1 tumors. D, Clodrolip treatment decreased lung metastasis of 4T1 tumors growing in a pre-irradiated mammary tissue (20 Gy). Metastases were quantified 21 days after tumor initiation. Quantification of $CD11b^+$ was done by flow cytometry, and $F4/80^+$ by image analysis. *p < 0.05, **p < 0.01and ***p < 0.001. n ≥ 5 mice per group. Results represent mean values ± SEM.

Figure 3. Hypoxia-induced KitL expression promotes metastasis. A, Hypoxia (0.1% O_2, 24 hours) increased KitL protein release in 4T1 cell culture supernatant, which was inhibited by the HIF1-inhibitor NSC-134754 but not vehicle only (DMSO). B, 4T1 tumors growing in pre-irradiated mammary tissue (20 Gy) expressed higher KitL protein levels and treatment with NSC-134754 (NSC) prevented this increase. C, Elevated plasma KitL levels in mice bearing 4T1 tumors growing in pre-irradiated mammary tissue (20 Gy) relative to control mice (0 Gy). D, KitL-silencing (KitL-KD) suppressed lung metastasis of 4T1 tumors growing in pre-irradiated mammary tissue (20 Gy). Representative HE stained sections of corresponding lungs are shown (bar: 1 mm). *p < 0.05, **p < 0.01 and ***p < 0.001. n ≥ 5 per group. Results represent mean values ± SEM.

Figure 4. KitL mediates radiation-induced mobilization of c-Kit^+ myeloid cells. A, c-Kit was expressed on a small fraction of bone marrow and blood-circulating cells of tumor-bearing mice but not on 4T1 cells i*n vitro* or *in vivo*. Dotted line: staining by isotype control antibody. B, Myeloid c-Kit^+ cells circulated at higher levels in the blood of mice bearing 4T1 tumor implanted in pre-irradiated mammary tissue (20 Gy) compared to non-irradiated mice (0 Gy). C, KitL silencing in 4T1 cells (KitL-KD) or

NSC-134754 (NSC) treatment decreased the number of circulating c-Kit$^+$ cells in mice bearing 4T1 tumor implanted in a pre-irradiated mammary tissue (20 Gy). DMSO, vehicle control treatment.

Figure 5. Mobilized CD11b$^+$c-Kit$^+$ cells home to tumors. A, CD11b$^+$GFP$^+$ isolated from 4T1 tumor-bearing, pre-irradiated, GFP$^+$BALB/c mice were adoptively transferred to mice bearing 4T1 tumors implanted in pre-irradiated mammary tissues. Six hours after injection GFP$^+$CD11b$^+$ cells were detected in the blood and tumor. In the blood they partially retained (25%) c-Kit expression, while in the tumor they lost it. B, KitL silencing in 4T1 cells decreased CD11b$^+$ cells in tumors growing in pre-irradiated mammary tissue (20 Gy) compared to non-irradiated mice (0 Gy). C, CD11b$^+$GFP$^+$ cells isolated as in experiment of panel (A) were transferred into tumor-bearing mice at a pre-metastatic stage. Six hours after injection, GFP$^+$CD11b$^+$ cells were detected in the lungs where they partially retained (25%) c-Kit expression. D, Increased frequency of GFP$^+$CD11b$^+$ was detected in pre-metastatic lungs of mice bearing tumors growing in pre-irradiated mammary tissue (20 Gy) compared to non-irradiated mice (0 Gy). KitL silencing in 4T1 cells (KitL-KD) significantly decreased their level. NS, non-silencing control. Cell analysis was performed by flow cytometry. *$p < 0.05$, **$p<0.01$ and ***$p < 0.001$. $n \geq 5$ mice per group. Results represent mean values ± SEM.

Figure 6. C-Kit inhibition reduces CD11b$^+$c-Kit$^+$ cell mobilization and attenuates radiation-induced metastasis. A, Adoptive transfer of total mononuclear cells isolated from mice bearing 4T1 tumors growing in pre-irradiated mammary tissue into control mice implanted with 4T1 cells, increases lung metastasis. Depletion of c-Kit$^+$

cells in adoptively transferred PBMCs attenuated this effect by approximately 50%. B, Treatment of pre-irradiated, tumor-bearing mice with the anti-c-Kit mAb ACK2 reduced the level of c-Kit$^+$ cells in the blood (left panel) and of CD11b$^+$ cells in the tumor (right panel). C, Treatment of pre-irradiated tumor-bearing mice with the anti-c-Kit mAb ACK2 (upper panel) or with the tyrosine kinase inhibitor nilotinib (lower panel) significantly reduced lung metastasis. Control, vehicle only treatment. *$p < 0.05$ and **$p < 0.01$. $n \geq 5$ per group. Results represent mean values ± SEM. D, Working model of the identified mechanism promoting radiation-induced lung metastasis. Radiation-mediated inhibition of tumor angiogenesis causes tumor hypoxia, which induces KitL expression. Released KitL mobilizes CD11b$^+$c-Kit$^+$ cells that home to the tumor and lung to promote tumor metastasis.

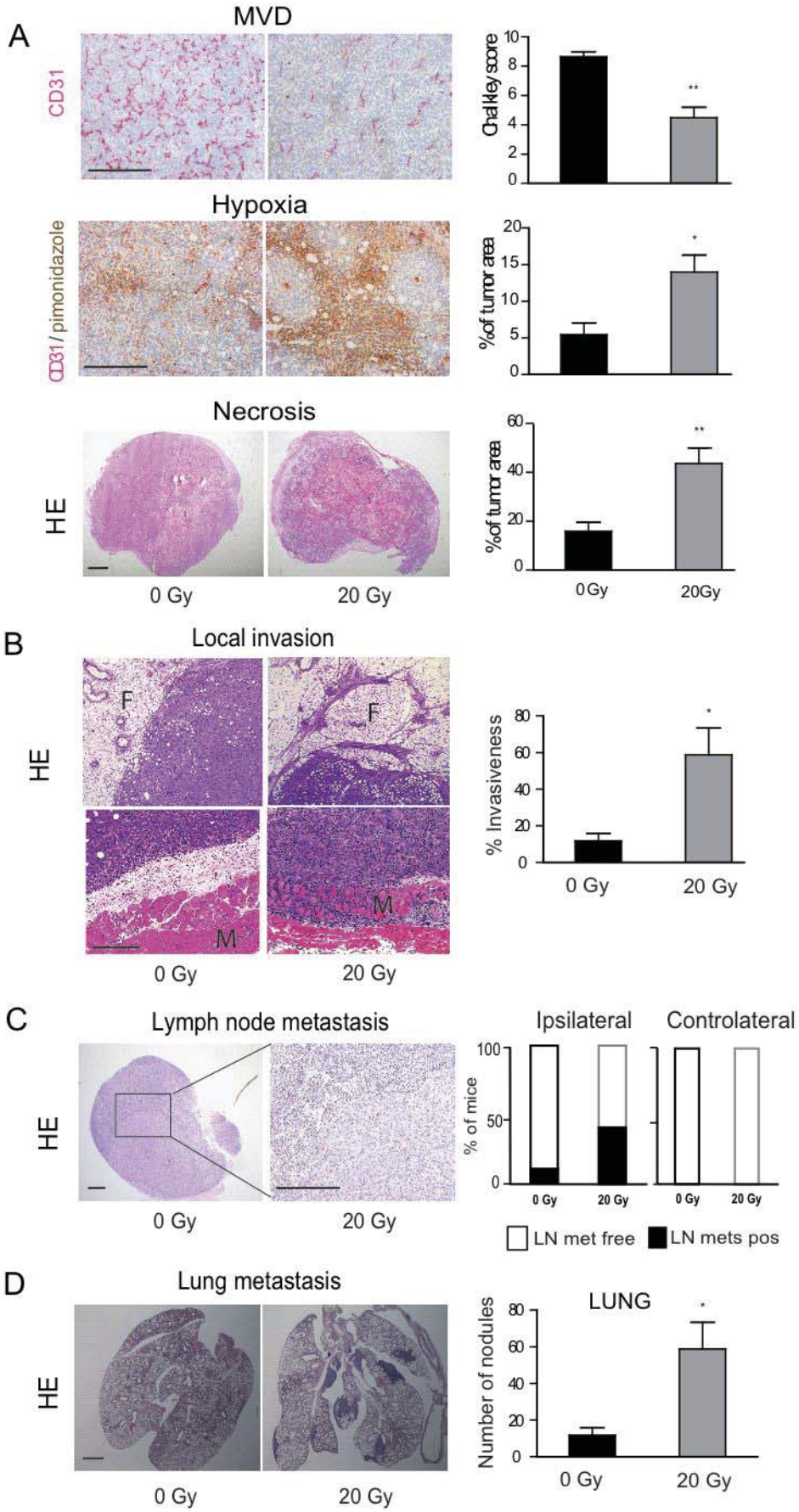

Fig. 1

Kuonen et al.

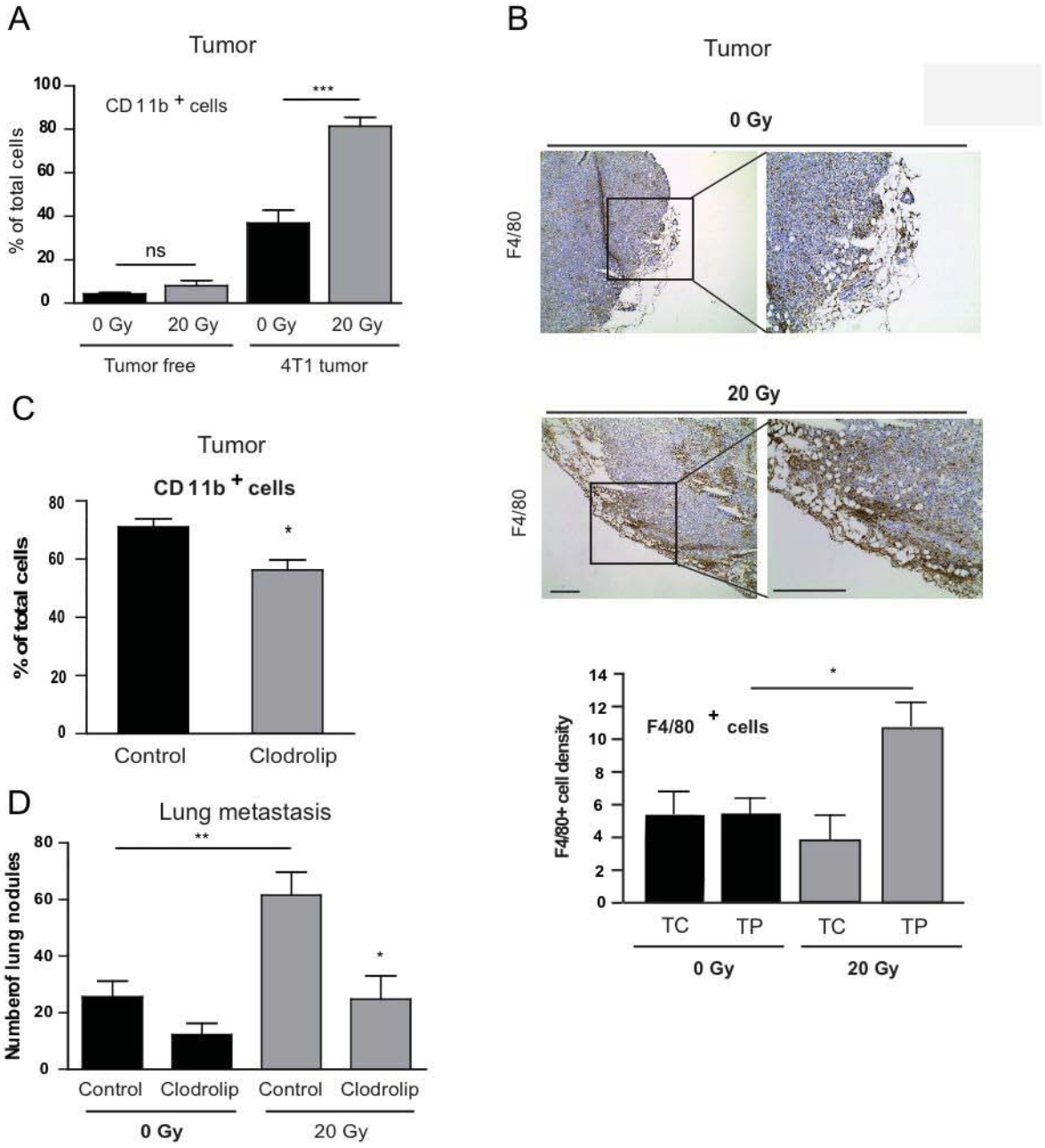

Fig. 2

Kuonen et al.

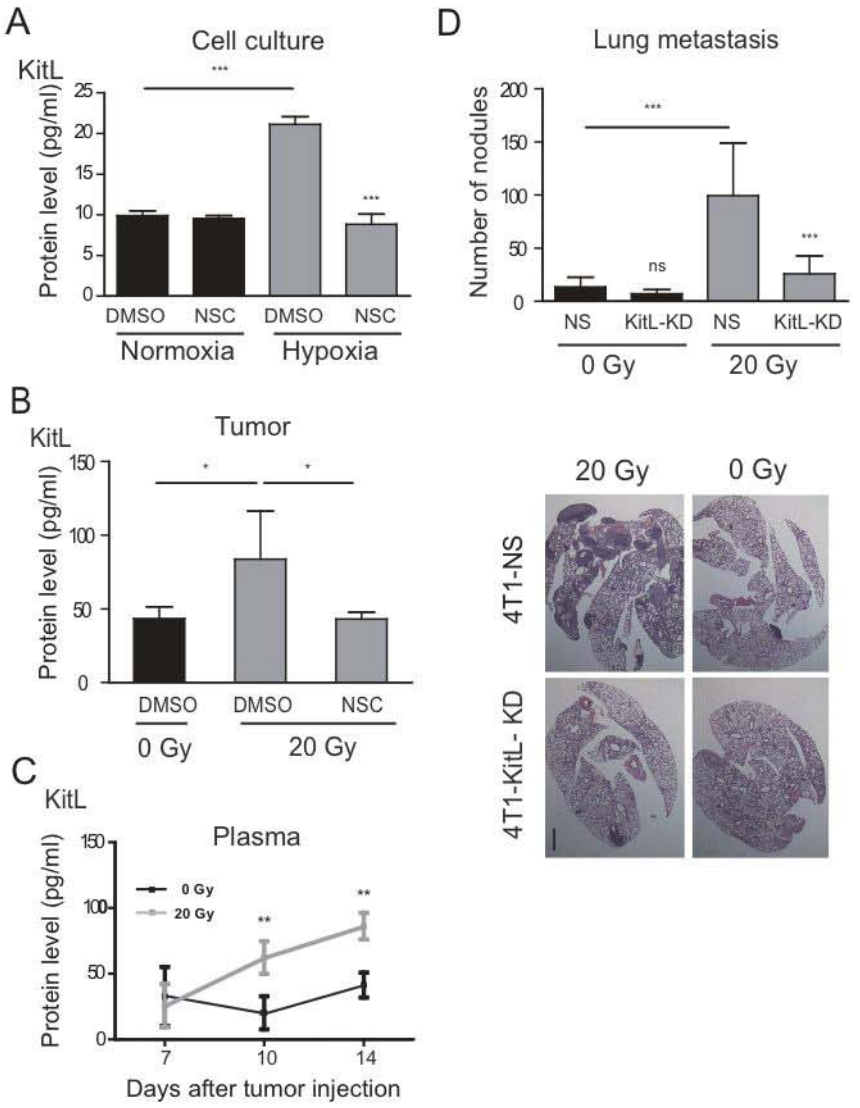

Fig. 3

Kuonen et al.

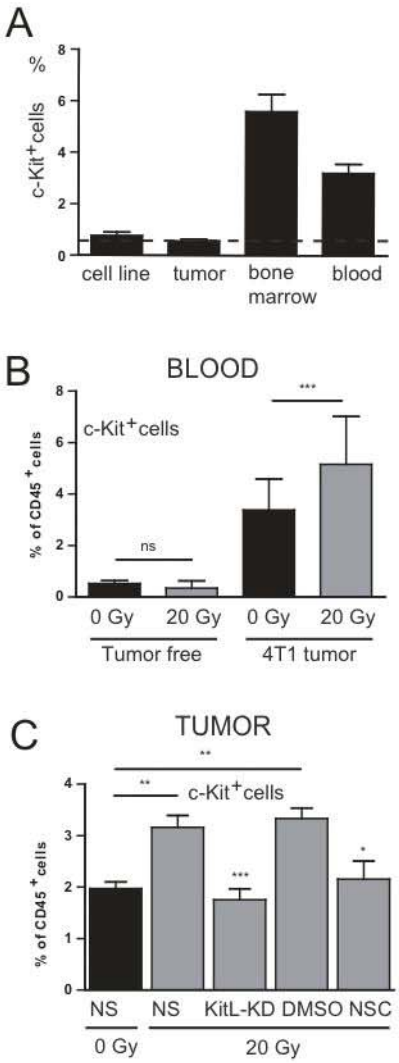

Fig. 4

Kuonen et al.

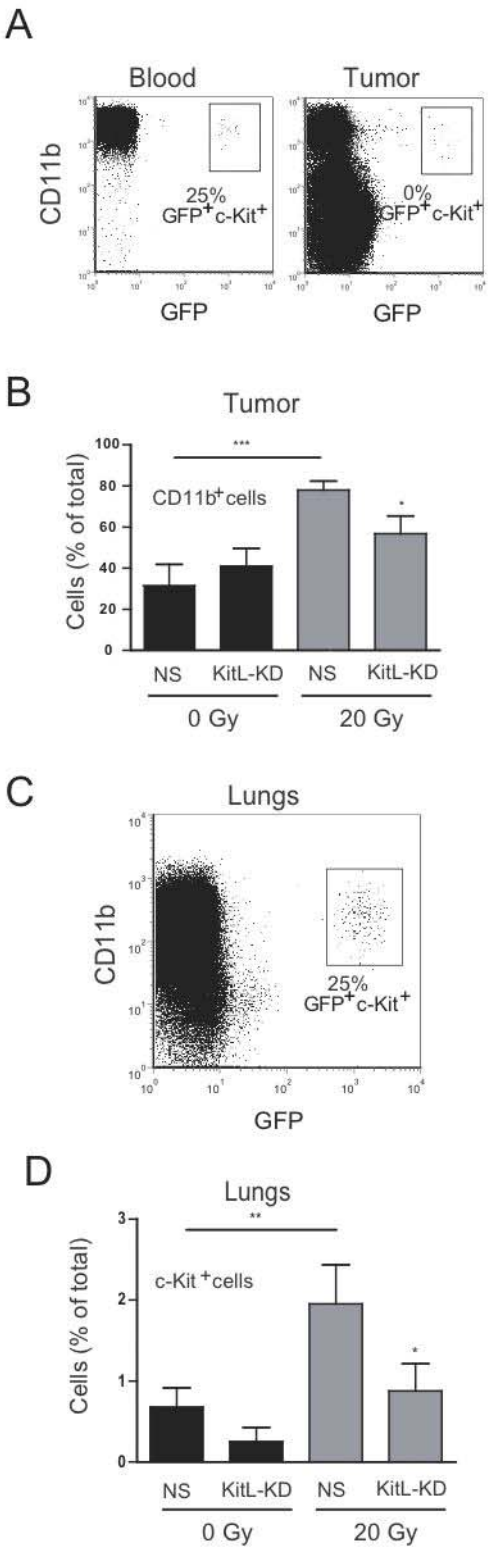

Fig. 5

Kuonen et al.

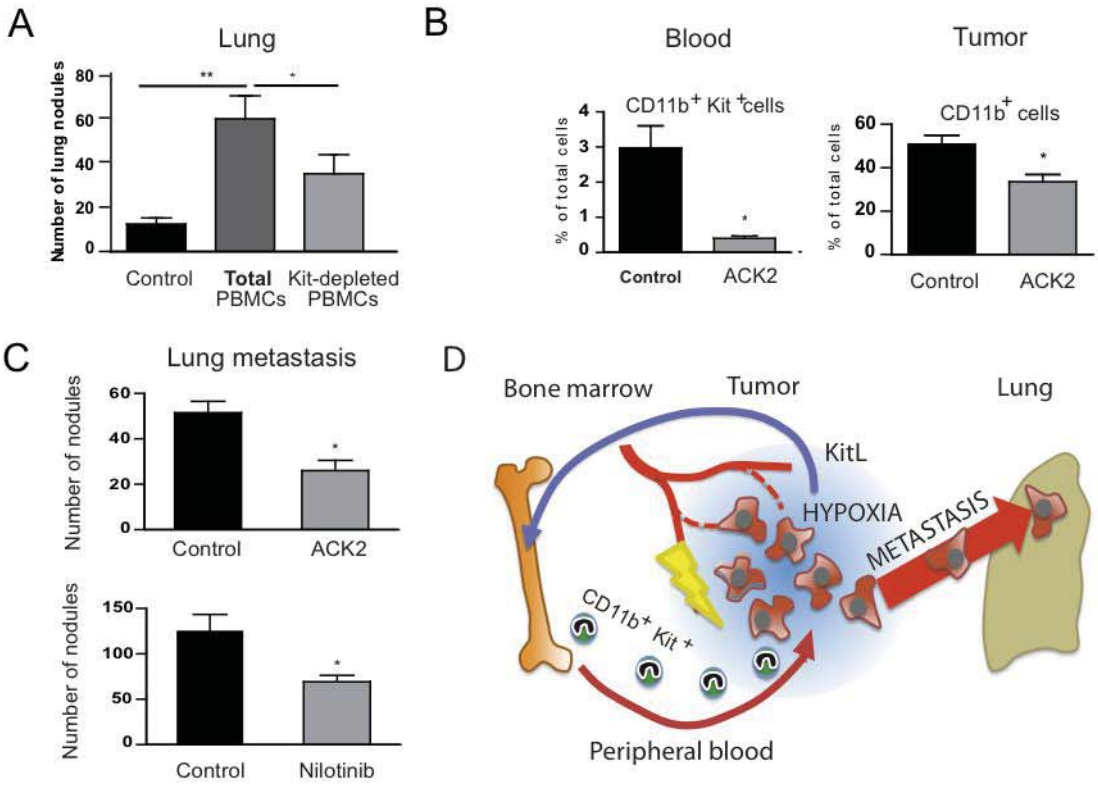

Fig. 6

Kuonen et al.